Fluorescence lifetime of normal, benign, and malignant thyroid tissues

Mariana Brandao
Ricardo Iwakura
Fagne Basilio
Kaique Haleplian
Amando Ito
Luiz Carlos Conti de Freitas
Luciano Bachmann

Fluorescence lifetime of normal, benign, and malignant thyroid tissues

Mariana Brandao,[a,*] Ricardo Iwakura,[b] Fagne Basilio,[b] Kaique Haleplian,[a] Amando Ito,[a] Luiz Carlos Conti de Freitas,[b] and Luciano Bachmann[a]

[a]Universidade de São Paulo, Faculdade de Filosofia, Ciências e Letras de Ribeirão Preto, Departamento de Física. Avenue Bandeirantes 3900, Ribeirão Preto, São Paulo 14040-901, Brazil

[b]Universidade de São Paulo, Faculdade de Medicina de Ribeirão Preto, Departamento de Oftalmo, Otorrino e Cirurgia de Cabeça e Pescoço, Avenue Bandeirantes 3900, Ribeirão Preto, São Paulo 14040-901, Brazil

Abstract. Fine-needle aspiration cytology is the standard technique to diagnose thyroid pathologies. However, this method results in a high percentage of inconclusive and false negatives. The use of time-resolved fluorescence techniques to detect biochemical composition and tissue structure alterations could help to develop a portable, minimally invasive, and nondestructive method to assist during surgical procedures. This study aimed to use fluorescence lifetimes to differentiate healthy and benign tissues from malignant thyroid tissue. The thyroid tissue was excited at 298–300 nm and the fluorescence decay registered at 340 and 450 nm. We observed fluorescence lifetimes at 340 nm emission of 0.80 ± 0.26 and 3.94 ± 0.47 ns for healthy tissue; 0.90 ± 0.24 and 4.05 ± 0.46 ns for benign lesions; and 1.21 ± 0.14 and 4.63 ± 0.25 ns for malignant lesions. For 450 nm emissions, we obtain lifetimes of 0.25 ± 0.18 and 3.99 ± 0.39 ns for healthy tissue, 0.24 ± 0.17 and 4.20 ± 0.48 ns for benign lesions, 0.33 ± 0.32 and 4.55 ± 0.55 ns for malignant lesions. Employing analysis of variance, we differentiate malignant lesions from benign and healthy tissues. In addition, we use quadratic discriminant analysis to distinguish malignant from benign and healthy tissues with an accuracy of 76.1%, sensitivity of 74.7%, and specificity of 83.3%. These results indicate that time-resolved fluorescence can assist medical evaluation of thyroid pathologies during surgeries. © *2015 Society of Photo-Optical Instrumentation Engineers (SPIE)*
[DOI: 10.1117/1.JBO.20.6.067003]

1 Introduction

At present, thyroid lesion diagnosis depends on the pathology results of fine-needle aspiration cytology obtained by examining stained sections by light microscopy. However, this method cannot effectively differentiate between benign and malignant follicular lesions. Thus, the rate of false-negative results for thyroid injuries is high.[1–4] Most of the surgeons rely upon gross inspection of size, hardness, and texture of the lesions to select thyroid tissues to send to pathologists for fast frozen section diagnosis during surgery. These fast frozen section results influence the type of thyroidectomy and the extent of the thyroid surgery. However, a large number of patients undergo unnecessary extensive operations or reoperation because only final histopathology can obtain the correct diagnosis of thyroid lesions. Therefore, finding new methods to provide information of biochemical composition and structure is critical to improve the prognosis of thyroid diseases.

Optical tissue diagnosis mediated by fiber-optic probes can perform noninvasive or minimally invasive real-time assessment of tissue pathology during the surgical procedure. In this regard, the use of time-resolved fluorescence techniques to detect alterations in the biochemical composition and structure of thyroid tissue could lead to a portable, minimally invasive and nondestructive methodology. One main advantage of this technique is that the fluorescence time decay does not alter when the fluorescence intensity changes.

This study aimed to determine lifetime fluorescence of benign and malignant thyroid lesions and to search for a technique to differentiate benign and malignant follicular lesions.

2 Methods

2.1 Sample Preparation

This study used 59 human thyroid samples, obtained from the University Hospital of the Ribeirão Preto Medical School, University of São Paulo. It included 34 patients from both genders with thyroid diseases who had undergone surgery. The Ethics Committee of the University Hospital of the Ribeirão Preto Medical School, University of São Paulo, approved the study and all patients signed a written informed consent to participate in the study.

The thyroid samples were removed during surgery and kept in phosphate-buffered saline. Each sample was bisected: half was sent for optical measurement and the other half for pathological analysis. The measurements of 41 samples were performed less than 2 h after surgical procedures. However, 18 samples were frozen in a low temperature freezer after the surgery. Later, these 18 samples were kept at room temperature to defrost for 30 min and all measurements were performed less

*Address all correspondence to: M.P. Brandao, E-mail: mpbrandao@gmail.com

than 2 h after removal from the freezer. We performed principal component analysis on the lifetime spectra of all results (divided by diagnostic groups: healthy, benign, and malignant) and established no statistical difference due to preparation between samples measured fresh and after defrosting. In addition, we performed analysis of variance (ANOVA) analysis on the lifetimes obtained for fresh and frozen samples (divided by diagnostics groups) using Fisher's least significant difference (LSD) and Tukey methods. The results showed no statistical difference between fresh and frozen samples for each diagnostic group (healthy, benign, and malignant).

Pathological analysis revealed that among these samples 13, 36, and 10 referred to healthy, benign, and malignant thyroid tissues, respectively. Benign samples included goiter, Hashimoto's thyroiditis, hyperplasia, benign tumor, and Hürthle cells adenoma; malignant samples comprised papillary carcinoma and follicular papillary carcinoma.

2.2 Time-Resolved Fluorescence Spectroscopy

The fluorescence intensity decay was measured on the basis of time-correlated single-photon counting. The excitation source was a Tsunami 3950 Spectra Physics titanium–sapphire laser that was tunable between the wavelengths of 840 and 1000 nm and which emitted 6 ps pulses, pumped by the solid-state laser Millenia X Spectra Physics with an emission at 530 nm. The pulse repetition rate was set to 8 MHz by using a 3980 Spectra Physics pulse picker. The laser was tuned so that a second- and third-harmonic generator (GWN-23PL Spectra Physics) gave an emergent beam tuned in the ranges of 420–500 nm and 280–333 nm. The output pulses were coupled to the optical fiber of a fluorescence probe (R400-7-UV-Vis, Ocean Optics); the probe tip was positioned

above the selected sample for excitation with a gap of approximately 1 mm. The six-fiber bundle of the probe collected the fluorescence and directed the light to an Edinburgh FL900 spectrometer. A refrigerated Hamamatsu R3809U microchannel plate photomultiplier detected the emitted photons. The optical fiber arrangement was used to obtain the instrument response function by collecting the scattered light at the same wavelength of excitation. The full width at half maximum of the instrument response function was typically 100 ps and the time resolution was 12 ps per channel. No significant background was observed in the experiments and software provided by Edinburgh Instruments was employed for analysis of the individual decays, which were fitted to multiexponential curves: $I(t) = \sum_i \alpha_i \exp[-t/\tau_i]$, where α_i are the pre-exponential factors and τ_i are the lifetimes. We judged the quality of the fit by analyzing the statistical parameter reduced-χ^2 (which average was 1.23) and by inspecting the residuals' distribution.

Samples were excited at 298–300 nm and the fluorescence intensity decay registered at 340 and 450 nm. The high fluorescence intensity at 340 nm enabled us to obtain decay times for all the 59 samples at this wavelength. However, the low absorption rate at the excitation wavelength of the fluorophores that fluoresced at 450 nm allowed us to obtain reliable decay times only for 35 samples (among these samples 8, 19, and 8 referred to healthy, benign, and malignant thyroid tissues, respectively).

We measured each sample at three different positions and obtained the fluorescence time decay for each of these measurements. In all cases, the decay profile intensity was fitted to a three-exponential decay using reconvolution with the instrument response function [Fig. 1(a)] and a short lifetime component below 0.1 ns was obtained with minor contribution to the
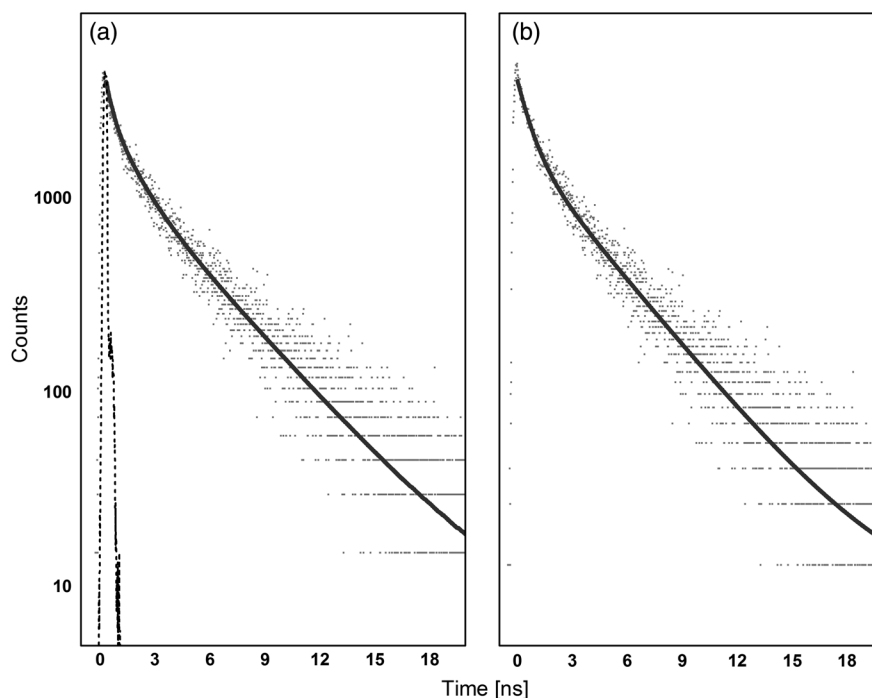
Fig. 1 Time-resolved fluorescence results for thyroid samples. (a) Decay profile for normal thyroid tissue (dotted lines), instrument response function (dashed lines), and three-exponential fitting of the decay profile reconvoluted with the instrument response function (solid lines). (b) Decay profile for normal thyroid tissue (dotted lines) and two-exponential tail fitting of the decay profile (solid lines). Note the log scale of the y-axis.

total emission (typically less than 5% contribution). We also made the fit from the decay profile without the initial transient points, a good fit was obtained with a two-exponential decay function [Fig. 1(b)], and the short lifetime component was absent. From the results of both procedures for the fit of experimental decays, we calculated the mean lifetime, using the definition of mean values: $\langle \tau \rangle = \sum_i \alpha_i \tau_i^2 / \sum_i \alpha_i \tau_i$.

The results for all the samples studied showed that the mean lifetimes obtained from the deconvolution differed by less than 1% from those of tail fit.

2.3 Data Processing

In the data processing, we preferred to use the values from tail fitting with a two-exponential decay curve for all the measurements, thus having the lowest number of parameters in the analysis. For each emission (340 and 450 nm), the differences in the decay values τ_1 and τ_2 between different tissue diagnostics (healthy, benign, and malignant) were analyzed by one-way ANOVA using Fisher's LSD, Tukey, and Dunnet methods. The control group for the Dunnet method was the healthy group.

We also performed a quadratic discriminant analysis of the decays' values using two groups: one group contained the malignant samples and the other group contained the healthy and benign samples. We used Minitab 16 Statistical® software to perform the quadratic discriminant analysis, which calculates the Mahalanobis distances using individual class covariance matrices. For cross validation, we used the leave-one-out method. This method works by omitting each data point one at a time, recalculating the classification function using the remaining data, and then classifying the omitted data point.

3 Results

Each individual decay shows a bi-exponential curve with a short lifetime near 1 ns and a long lifetime around 4.0 ns for fluorescence emissions at 340 and 450 nm. Table 1 presents the average values and standard deviation for each histopathology diagnosis.

At emission in 340 nm, the mean values of pre-exponential factors were circa 0.40 for the short lifetime and 0.60 for the long lifetime. At emission in 450 nm, the values were 0.64 and 0.26 for the short and long lifetimes, respectively. The use of pre-exponential factors for discrimination analysis presented no significant difference between tissues. On the

other hand, from the fluorescence lifetimes, we observed that malignant samples yielded larger lifetime values when compared to healthy and benign samples for both emission wavelengths. However, the benign and healthy samples were similar for both short and long lifetimes. Figure 2 shows the scattered plot with the short [Fig. 2(a)] and long [Fig. 2(b)] lifetime values corresponding to healthy, benign, and malignant thyroid tissues for 340 nm emission.

From the set of decays corresponding to a given class of tissue (healthy, benign, or malignant), we calculated the mean values of the short (τ_1) and the long (τ_2) lifetimes and analyzed by one-way ANOVA using Fisher's LSD, Tukey, and Dunnet methods. Table 2 presents the results for ANOVA using Fisher's LSD and Tukey methods.

The Fisher's LSD method distinguishes the three different groups for the short lifetime (τ_1) at 340 nm emission. Also, for both lifetimes (τ_1 and τ_2) the results of Fisher's LSD and Tukey methods exhibited a statistical difference between healthy and malignant groups. However, the statistical analyses between healthy and benign groups for τ_2 present no difference with both methods at 340 nm emission.

For fluorescence emissions at 450 nm, both methods presented the same results. No statistical difference exists between the healthy, benign, and malignant groups on the short lifetimes (τ_1). A statistical difference between healthy and malignant groups occurred on longer lifetimes (τ_2), but not between healthy and benign groups. Table 3 contains the results for ANOVA using Dunnet method.

The Dunnet method at 340 nm presented a statistical difference between healthy and malignant groups for both lifetimes. However, the statistical analysis shows that healthy and benign groups are similar. For emissions at 450 nm, the long lifetimes presented a statistical difference between healthy and malignant groups, but not between healthy and benign groups. Once more, we found no statistical difference between the short lifetimes at 450 nm emission.

Table 4 displays the comparison between a time-resolved fluorescence technique and the histopathologic diagnosis by discriminant analysis (described at Sec. 2.3) using the short (τ_1)
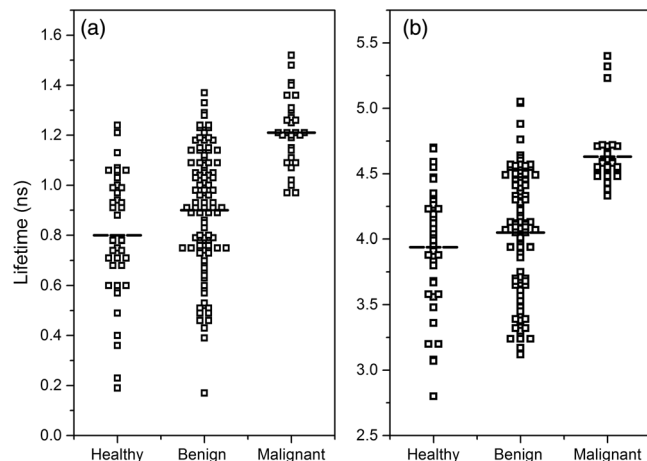
Fig. 2 Scattered plot of lifetimes' values for healthy, benign, and malignant thyroid tissues measured for 340 nm emission. (a) Short lifetimes (black square containing white square) and its average value (dashed lines). (b) Long lifetimes (black square containing white square) and its average value (dashed lines).

Table 1 Average fluorescence lifetime values for healthy, benign, and malignant thyroid samples excited at 300 nm and measured at 340 and 450 nm.

Emission (nm)	Histopathology diagnosis	τ_1 (ns)	τ_2 (ns)
340	Healthy	0.80 ± 0.26	3.94 ± 0.47
	Benign	0.90 ± 0.24	4.05 ± 0.46
	Malignant	1.21 ± 0.14	4.63 ± 0.25
450	Healthy	0.25 ± 0.18	3.99 ± 0.39
	Benign	0.24 ± 0.17	4.20 ± 0.48
	Malignant	0.33 ± 0.32	4.55 ± 0.55

Table 2 Analysis of variance (ANOVA) analyses by Fisher's least significant difference (LSD) and Tukey methods of the fluorescence time decay for healthy, benign, and malignant thyroid samples excited at 300 nm and measured at 340 and 450 nm. In the last column, the same letters denote nonstatistical difference; {A,B,C} is used to indicate the group classification. This comparison is valid for each method and lifetime separately.

Emission (nm)	Decay	P value	Method	Simultaneous confidence (%)	Individual confidence (%)	Histopathology diagnosis	Mean (ns)	Group
340	τ_1	<0.001	Fisher's LSD	95	87.82	Healthy	0.8013	**C**
						Benign	0.8993	**B**
						Malignant	1.214	**A**
			Tukey	98.07	95	Healthy	0.8013	**B**
						Benign	0.8993	**B**
						Malignant	1.214	**A**
	τ_2	<0.001	Fisher's LSD	95	87.82	Healthy	3.9351	**B**
						Benign	4.0536	**B**
						Malignant	4.6283	**A**
			Tukey	98.07	95	Healthy	3.9351	**B**
						Benign	4.0536	**B**
						Malignant	4.6283	**A**
450	τ_1	0.230	Fisher's LSD	95	87.86	Healthy	0.2490	**A**
						Benign	0.2375	**A**
						Malignant	0.3296	**A**
			Tukey	98.07	95	Healthy	0.2490	**A**
						Benign	0.2375	**A**
						Malignant	0.3296	**A**
	τ_2	0.001	Fisher's LSD	95	87.82	Healthy	3.9935	**B**
						Benign	4.2019	**B**
						Malignant	4.5509	**A**
			Tukey	98.07	95	Healthy	3.9935	**B**
						Benign	4.2019	**B**
						Malignant	4.5509	**A**

and the long (τ_2) lifetimes as predictors. The results show a good accuracy and proportion of correct malignant classification by both lifetimes at 340 nm emissions. For 450 nm emission, although the accuracy is higher than 65% for all predictors, the proportion of correctly classified malignant samples is poor.

4 Discussion

The optical characteristics of fluorophores depend on the properties of the medium, such as pH and temperature, and its ligands. Therefore, it is difficult to directly compare the lifetime fluorescence observed for thyroid samples with those of tissues with similar chromophore constituents,[5–10] even though it is possible to correlate and expect similar peak positions and lifetimes

values as observed by the literature for healthy soft tissue. The fluorescence emitted at 340 nm, while exciting the sample in the 285–300 nm region, can correspond to elastin and tryptophan fluorescence.[5–9] The fluorescence at 450 nm emission, while exciting the sample in the 285–300 nm region, can correspond to NADH-protein, and NADH-free.[5–7]

The results of Tables 1 and 2 show larger values of fluorescence lifetimes for malignant samples when compared to healthy and benign samples. The ANOVA results for emissions at 340 nm exhibited a statistical difference between healthy and malignant groups for Fisher's LSD, Tukey, and Dunnet methods for both lifetimes. However, the short lifetime for emissions at 450 nm did not present a statistical difference between the histopathological groups for all three ANOVA methods.

Table 3 ANOVA analyses by Dunnet method of the fluorescence time decay for healthy, benign, and malignant thyroid samples excited at 300 nm and measured at 340 and 450 nm. The control group for the Dunnet method was the healthy group and the family error was set to 0.05. In the last column, results not labeled with the letter "A" are significantly different from the control group. This comparison is valid for each lifetime separately.

Emission (nm)	Individual error	Critical value	Decay	P value	Histopathology diagnosis	Mean (ns)	Group
340	0.0276	2.22	τ_1	<0.001	Healthy (c)	0.8013	**A**
					Benign	0.8993	
					Malignant	1.214	
			τ_2	<0.001	Healthy (c)	3.9351	**A**
					Benign	4.0536	**A**
					Malignant	4.6283	
450	0.0283	2.23	τ_1	0.230	Healthy (c)	0.2490	**A**
					Benign	0.2375	**A**
					Malignant	0.3296	**A**
			τ_2	0.001	Healthy (c)	3.9935	**A**
					Benign	4.2019	**A**
					Malignant	4.5509	

Note: Groups not labeled with letter A are significantly different from control level mean. (c)= control group.

Table 4 Comparison of the results between lifetimes and histopathologic examination by discriminant analysis using quadratic function between two groups: healthy and benign, and malignant.

Emission (nm)	Predictors	Hispathologic diagnosis	True group			% of correct classified
			Benign and healthy	Malignant	Total	
340	τ_1 and τ_2	Benign and healthy	109	37	146	74.7
		Malignant	5	25	30	83.3
				Total accuracy		76.1
	τ_1	Benign and healthy	103	43	146	70.5
		Malignant	4	26	30	86.7
				Total accuracy		73.3
	τ_2	Benign and healthy	102	44	146	69.9
		Malignant	2	28	30	93.3
				Total accuracy		73.9
450	τ_1 and τ_2	Benign and healthy	51	21	72	70.8
		Malignant	11	12	23	52.2
				Total accuracy		66.3
	τ_1	Benign and healthy	63	9	72	87.5
		Malignant	19	4	23	17.4
				Total accuracy		70.5
	τ_2	Benign and healthy	55	17	72	76.4
		Malignant	13	10	23	43.5
				Total accuracy		68.4

The discriminant analysis was able to distinguish the malignant samples with 76.1% when using both lifetimes as predictors for 340 nm emissions. It achieved an 83.3% correct classification for malignant samples when using both lifetimes as predictors and 93.3% of correct classification for malignant samples when using only the longer lifetimes as predictor.

The poor results obtained at 450 nm emissions maybe caused by the low absorption rate at the excitation wavelength. We believe that applying different wavelengths can greatly improve the results achieved for this emission.

Recent studies have connected cancer with tryptophan metabolism activation so that the malignancy evades immune control and suggest that tryptophan may serve as a marker to monitor disease activity.[10–14] The lifetime of tryptophan in neutral aqueous solution excited at 280 nm for emissions at 340 nm is 0.67 ± 0.12 and 3.17 ± 0.04 ns.[9] Table 1 presented lifetime fluorescence measurements for the healthy thyroid samples at 340 nm of 0.80 ± 0.26 and 3.94 ± 0.47 ns. Malignant thyroid samples yielded larger lifetime values at 340 nm of 1.21 ± 0.14 and 4.63 ± 0.25 ns. The tryptophan metabolic pathway could be the cause for these longer lifetimes for malignant thyroid samples while recording fluorescence emissions at 340 nm. However, any direct correlation is inadequate because the fluorescence lifetime is a mean value of all fluorophores presented in the thyroid tissue fluorescing at 340 nm.

5 Conclusions

This study has successfully demonstrated that fluorescence lifetimes at 340 nm emission can differentiate between thyroid malignant and healthy/benign tissues. It indicates fluorescence lifetime as a promising technique for application as real-time assessment for thyroid lesions during the surgical procedure. Future studies are still necessary to correlate the lifetimes and the histopathological diagnosis for all thyroid pathologies, specially the follicular lesions, and the application of different excitation wavelengths may reveal the effects of other fluorophores on cancerous tissues.

References

1. P. Rout and S. Shariff, "Diagnostic value of qualitative and quantitative variables in thyroid lesions," *Cytopathology* **10**(3), 171–179 (1999).
2. C. S. Teixeira et al., "Thyroid tissue analysis through Raman spectroscopy," *Analyst* **134**(11), 2361–2370 (2009).
3. M. J. Pitman et al., "The fluorescence of thyroid tissue," *Otolaryngol. Head Neck Surg.* **131**(5), 623–627 (2004).
4. G. Giubileo et al., "Fluorescence spectroscopy of normal and follicular cancer samples from human thyroid," *Spectroscopy* **19**(2), 79–87 (2005).
5. M. Y. Berezin and S. Achilefu, "Fluorescence lifetime measurements and biological imaging," *Chem. Rev.* **110**(5), 2641–2684 (2010).
6. L. Marcu, "Fluorescence lifetime techniques in medical applications," *Ann. Biomed. Eng.* **40**(2), 304–331 (2012).
7. L. Bachmann et al., "Fluorescence spectroscopy of biological tissues: a review," *Appl. Spectrosc. Rev.* **41**(6), 575–590 (2006).
8. D. Chorvat, Jr. and A. Chorvatova, "Multi-wavelength fluorescence lifetime spectroscopy: a new approach to the study of endogenous fluorescence in living cells and tissues," *Laser Phys. Lett.* **6**(3), 175–193 (2009).
9. D. M. Rayner and A. G. Szabo, "Time resolved fluorescence of aqueous tryptophan," *Canadian J. Chem.* **56**(5), 743–745 (1978).
10. Y. Engelborghs, "The analysis of time resolved protein fluorescence in multi-tryptophan proteins," *Spectrochim. Acta* **57**(11), 2255–2270 (2001).
11. C. Goldman et al., "On the contribution of electron transfer reaction to the quenching of tryptophan fluorescence," *J. Chem. Phys.* **103**, 10614–10620 (1995).
12. M. Platten, W. Wick, and B. J. Van den Eynde, "Tryptophan catabolism in cancer: beyond IDO and tryptophan depletion," *Cancer Res.* **72**(21), 5435–5440 (2012).
13. C. A. Opitz et al., "An endogenous tumour-promoting ligand of the human aryl hydrocarbonreceptor," *Nature* **478**(7368), 197–203 (2011).
14. X. Liu et al., "Selective inhibition of IDO1 effectively regulates mediators of antitumor immunity," *Blood* **115**(17), 3520–3530 (2010).

Mariana Brandao is a postdoctoral researcher at the University of Sao Paulo. She received her BS and MS degrees in physics from the Federal University of Juiz de Fora in 2000 and 2004, respectively, and her PhD in physics from the Pontifical Catholic University of Rio de Janeiro in 2011. Her current research interests include biophysics, applied optics, and spectroscopy applied in medicine and biology.

Luiz Carlos Conti de Freitas has graduated in medicine from Federal University of Uberlandia, and received his master's degree in medicine and his PhD in medical sciences from University of Sao Paulo. He has experience in medicine, acting mainly on neck and head surgeries, foreign bodies, and esophagus and esophagoscopy.

Luciano Bachmann is a professor of the Physics Department at the University of Sao Paulo. He received his BSc degree in physics from the Federal University of Santa Catarina, and his master's and PhD in physics in the Institute of Nuclear Energy Research at University of Sao Paulo. He has experience in the area of physics, with emphasis on condensed matter. He focused mainly on biophysics, enamel and dentin, optical properties and chemical composition of organic matter, and crystallography.

Biographies for the other authors are not available.